Desalination and Water Treatment
www.deswater.com

doi: 10.5004/dwt.2018.21949

108 (2018) 40–48
March

Porous P84 co-polyimide anion exchange membranes for diffusion dialysis application to recover acids

Pin Wang[a], Cuiming Wu[a,*], Mengjie Sun[a], Xu Zhang[a,*], Yonghui Wu[b]

[a]*Anhui Key Lab of Controllable Chemical Reaction & Material Chemical Engineering, School of Chemistry and Chemical Engineering, Hefei University of Technology, Hefei 230009, China, Tel. +86-0551-62901458; email: cmwu@ustc.edu.cn (C. Wu), Tel. +86-0551-62901450; email: xzhang@hfut.edu.cn (X. Zhang), Tel. +86-18356065613; email: 18356065613@163.com (P. Wang), Tel. +86-18756933962; email: 841936089@qq.com (M. Sun)*
[b]*School of Chemistry and Environmental Engineering, Yancheng Teachers University, Yancheng 224002, China, Tel. +86-15895198337; email: wuyonghui1000@126.com*

Received 14 August 2017; Accepted 24 January 2018

ABSTRACT

Porous anion exchange membranes based on P84 co-polyimide are prepared by phase inversion process and applied to recover acids through diffusion dialysis (DD) for the first time. Recovery efficiency of sulfuric acid (H_2SO_4) from simulated titanium white waste liquor (H_2SO_4/$FeSO_4$ mixture), as well as the volume of water osmosis from diffusate (low concentration solution) to dialysate (high concentration solution), is determined by membrane morphologies and operation temperature. In addition, the optimized membrane is also tried to operate DD process of pure acetic acid (HAc). The optimized membrane, which is prepared by phase inversion in isopropanol, amination and then quaternization at 46°C, shows both high permeability and selectivity for H_2SO_4/$FeSO_4$ mixture. The dialysis coefficient of H_2SO_4 (U_H) is 0.0069 m/h and the separation factor (S) is as high as 53.8, while the volume of water osmosis is 27 mL. The dialysis coefficient of HAc (U_{HAc}) is in the range 0.00239–0.0133 m/h under operation temperature of 15°C–45°C, and the volume of water osmosis is maintained ~3 mL. The membranes are promising for acids recovery due to their high permeability and selectivity.

Keywords: P84 co-polyimide; Porous; Anion exchange membrane; Diffusion dialysis; Acid recovery; Water osmosis

1. Introduction

A large amount of acidic wastewater is produced from industrial processes such as metallurgy electrolysis, electroplating and acid pickling [1–3]. Direct discharge of the waste liquor not only wastes recyclable resources, but also constitutes a threat to the environment. For instance, titanium dioxide (TiO_2) which is widely used in plastics [4], paint [5], white pigment [6], sunscreen and cosmetics [7,8], is currently produced mainly through chloride process or sulfate process [9]. Moreover, sulfate process is more widely used due to the abundant, cheap and easily available raw materials (ilmenite and sulfuric acid), the mature technology, simple equipment and easy operation. However, a large amount of waste solution containing dilute sulfuric acid, ferrous sulfate and other sulfates is generated during the process [10]. Another example is the production of organic acids such as acetic acid (HAc), which has been widely used in foods, beverages, pharmaceuticals and cosmetics [11]. Generally, organic acids are produced by two commercially available methods: chemical synthesis from petroleum and fermentation, both of which include precipitation or extraction stages generating chemical wastewater with high salt content [12–14]. Many methods are adopted to reduce the impact of acidic wastewater on environment, such as distillation [15], cooling [16], ion exchange [17], solvent extraction [18] and membrane separation [19,20].

Diffusion dialysis (DD) is one of membrane separation processes, which is characterized by low energy

* Corresponding author.

consumption and environmentally friendly. Using anion exchange membrane (AEM) as an example, solute which is driven by concentration gradient, spontaneously passes through AEM from higher concentrate side to lower concentrate one [21]. As the core part of diffusion, AEM determines the ions transport rate and the separation performance. AEMs based on poly(2,6-dimethyl-1,4-phenylene oxide) (PPO; commercial name of DF-120), polysulfoxide (commercial name of S203) or polystyrene (commercial name of Neosepta-AFN) have been successfully applied in industry or laboratory for recovery of HCl from HCl/$FeCl_2$ [22–24]. Nevertheless, other acids such as H_2SO_4 and HAc are more difficult for recovery, due to the lower diffusivity and higher size of SO_4^{2-} and Ac^-. For instance, the proton dialysis coefficient (U_H) for HCl is 0.009 m/h at 25°C for DF-120 membrane [25], while the value for H_2SO_4 is about 0.0018 m/h for S203 membrane [23] and about 0.00234 m/h for DF-120 membrane (at 25°C) [26]. What's more, HAc is corrosive and can partially dissolve DF-120 membrane [27], and thus DD process of HAc is still rare in practical application.

To improve the acid permeability, porous membranes have been prepared by phase inversion of brominated PPO, followed by partial hydrolysis and quaternization steps [28]. The permeability for acid is markedly increased and the U_H value for HCl can be enhanced to 0.042 m/h. Unfortunately, the membranes are swelling seriously in water, as revealed by the high water content of 449.0%. Though the values can be decreased to 126.0%–169.5% through membrane modification by multisilicon copolymer [28], the preparation and preservation of the multisilicon copolymer are relatively complex, which increases the difficulty of their application in industrial process. Besides, the DD application using porous membranes for recovery of acids other than HCl has been rarely explored. [29–31].

Membrane material of polyimide (PI) has drawn our attention due to its excellent solvent resistance, high temperature resistance, outstanding mechanical properties and dielectric properties [32,33]. What's more, dense membranes based on PI have been widely used in gas separation [34] and penetration gasification [35,36], while the porous membranes are utilized for ultrafiltration [37], nanofiltration [38] and free-flow isoelectric focusing application [39]. Nevertheless, the PI membranes are seldom reported in DD application. Besides, the water osmosis, which is a common phenomenon in the process of DD and electrodialysis [40], is seldom investigated for porous membranes.

Hence, in this manuscript, porous P84 co-polyimide AEMs are prepared by phase inversion, and then used in DD to investigate HAc permeability and recover sulfuric acid from simulated titanium white waste acid. Porous structure can enhance the proton permeability, while water penetration from the low concentration to high concentration side can also be increased. Therefore, the water osmosis phenomenon may be more serious for porous membranes than traditional dense membranes. The water osmosis phenomenon of porous membranes is investigated in DD process under different operating temperatures. Also, the DD performances and water osmosis phenomenon are correlated with the membrane morphology and physicochemical properties.

2. Experimental

2.1. Materials

P84 co-polyimide with a molecular weight of 153 kDa was obtained from HP Polymer GmbH (Austria). Isopropanol (IPA), methanol, *N*-methylpyrrolidone (NMP), ferrous sulfate ($FeSO_4{\cdot}7H_2O$) and 98 wt% of concentrated sulfuric acid (H_2SO_4) were purchased from Sinopharm Chemical Reagent Co., Ltd. (China) and used without further purification. Anhydrous sodium carbonate (Na_2CO_3) from Sinopharm Chemical Reagent Co., Ltd. (China) was heated at 230°C–300°C for 3 h before use. Deionized water was used throughout the experiment.

2.2. Preparation of porous P84 co-polyimide membranes

Porous P84 co-polyimide membranes were prepared according to the previous method [41], and the procedures are shown in Fig. 1. The process mainly included three parts. (1) Phase inversion: P84 powder was stirred to dissolve in NMP with the concentration of 23 wt%. Then, the solution was cast onto a clean glass plate and then immediately immersed in non-solvent bath (IPA or water) at around 20°C. For IPA as the non-solvent, the membrane was taken out after 20 min, but for water, the membrane was taken out after 4 h. All the prepared membrane was then immersed in methanol for 2 h. (2) Amination: the P84 base membrane obtained by step (1) was soaked in a 5/5/90 (v/v) ethylene diamine/butyl diamine/methanol solution for 30 min. In this process, part of the diamine reacted for the cross-linkage, while the free $-NH_2$ group was retained for further ethylation to form quaternary amine groups. (3) Quaternization by ethylation: the membrane was immersed into a 30 wt% ethyl bromide/methanol solution for quaternization at 56°C or 46°C. The obtained membranes were named Mem-I-56 (IPA as non-solvent, quaternization at 56°C), Mem-I-46 (IPA, 46°C), Mem-W-56 (water as non-solvent, quaternization at 56°C) and Mem-W-46 (water, 46°C). In contrast, dense membrane was prepared by casting P84 co-polyimide solution and then drying under vacuum at 40°C for 12 h and heating at 60°C for 12 h, followed by amination and quaternization steps as mentioned above. The dense membrane was designated as Mem-D.

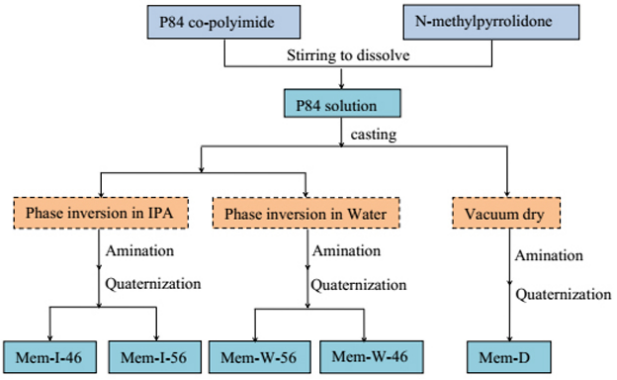

Fig. 1. The preparation procedures for P84 co-polyimide membranes.

2.3. Membrane characterization

Thermal stability was investigated by the thermogravimetric analysis (TGA), which was conducted by a Shimadzu TGA-50H analyzer under air flow with a heating rate of 10°C/min.

Chemical stability was investigated under the acidic condition to research the acid resistance of the obtained P84 membranes. The wet membrane samples were immersed in H_2SO_4 (1.0 mol/L) solution for 2 d at 25°C, and then the weight change (ΔW) was measured to observe the acid resistance.

$$\Delta W = \frac{W_1 - W_0}{W_0} \times 100\% \quad (1)$$

where W_1 is the sample mass after immersed in H_2SO_4 (1.0 mol/L) solution for 2 d at 25°C, and W_0 is initial wet sample mass.

Mechanical stabilities including tensile strength (TS) and the elongation at break (E_b) were measured using Instron Universal Tester (Model 2519-104) under an operating head load of 500 N. As the membranes were stored in aqueous solution, their surface water was removed with filter paper before testing. The width of the tested membranes was 10 mm and the test speed was 10 mm/min.

2.4. Diffusion dialysis

2.4.1. Apparatus

The self-configured dialyzer is schematically shown in Fig. 2, whose parameters are given in Table 1. The dialyzer has six channels, three of which are diffusate sides and filled with water, and the other three are dialysate sides and filled with the solution of $H_2SO_4/FeSO_4$ (0.9/0.3 mol/L) or HAc (0.9 mol/L). Five membrane sheets in the stack were separated by silicon rubber and plexiglas spacer with a thickness of around 10 mm. Two peristaltic pumps (BT600, Baoding Chuangrui Precision Pump Co., Ltd., China) circulated the feed (250 mL) and water (250 mL) to the corresponding compartments at 100 mL/min.

Running time of DD was fixed at 5 h. Experimental temperature was increased from 15°C, 25°C, 35°C to 45°C. After the running, the volume of dialysate compartment increased while the volume of diffusate compartment decreased, indicating the water osmosis from the diffusate to the dialysate. The volume changes of both dialysate and diffusate compartments were recorded and the average value was taken as the volume of water osmosis.

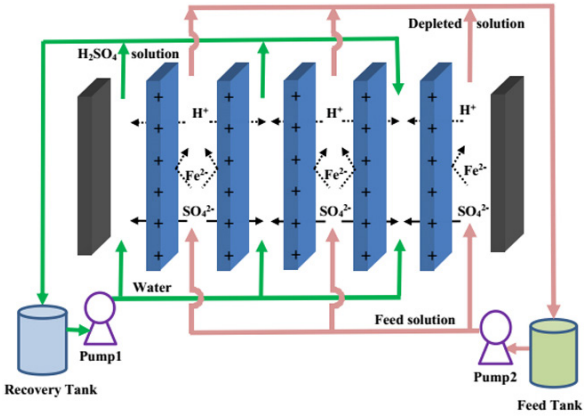

Fig. 2. Self-configured DD dialyzer for acid recovery, with $H_2SO_4/FeSO_4$ system as an example.

2.4.2. Methods and data calculations

H^+ ions concentration in the $H_2SO_4/FeSO_4$ mixture was determined by titration using 0.02 mol/L standard Na_2CO_3 solution with methyl orange as an indicator, while the Fe^{2+} ions concentration was determined by 1,10-Phenanthroline Spectrophotometry using UV-2401PC (Shimadzu Ltd., Japan) [42]. The concentration of HAc was directly determined by titration with NaOH solution. The dialysis coefficient (U), separation factor (S) and water osmosis volume (V_{H_2O}) were calculated as follows.

U can be calculated by the following formula [43]:

$$U = \frac{M}{At\Delta C} \quad (2)$$

where M is the amount of the component transported in moles, A is the total effective area of the membrane (100 cm^2), t is the operation time of the experiment (5 h) and ΔC is the logarithmic average concentration between the dialysate compartment and diffusate compartment in moles per cubic meters defined as:

$$\Delta C = \frac{C_f^0 - (C_f^t - C_d^t)}{\ln[C_f^0 / (C_f^t - C_d^t)]} \quad (3)$$

where C_f^0 and C_f^t are the dialysate concentrations at time 0 and t, respectively, and C_d^t is the diffusate concentration at time t.

The S value with respect to one species over another is given as the ratio of dialysis coefficients (U) of the two species present in the solution, and can be calculated as specified below.

$$S = \frac{U_H}{U_{Fe}} \quad (4)$$

Table 1
Parameters of the self-configured DD dialyzer

Item	Specifications
Membrane type	AEM based on P84 co-polyimide
Total effective membrane area (cm^2)	100
Number of membrane sheet	5
Distance between membranes (cm)	0.9
Dimension of membranes sheet	9.6 cm (L) × 5.3 cm (W) × (0.05–0.15 mm) (T)
Dimension of dialyzer stack	10.0 cm (L) × 8.0 cm (W) × 13.3 cm (H)

The water osmosis volume (V_{H_2O}) is calculated by the following equation:

$$V_{H_2O} = \frac{\left(V_f^t - V_f^0\right) + \left(V_d^0 - V_d^t\right)}{2} \quad (5)$$

where V_f^0 and V_f^t are the volume of dialysate compartment at time 0 and t, and V_d^0 and V_d^t are the volume of diffusate compartment at time 0 and t, respectively.

3. Results and discussion

3.1. Membrane morphology and properties

The membranes were prepared according to previously reported method [41]. Some of the basic physicochemical properties are cited and shown in Table 2, and the membrane thickness and chemical stability are measured in this research.

The SEM graphs have been shown previously [41] and the morphology difference can be briefly summarized as following: Mem-I-56 and Mem-I-46 which were prepared through phase inversion in IPA exhibit sponge-like structure over the whole cross-section, including a denser skin layer and a more porous supporting layer. The micronsized pores are separated by ultrathin walls, so that they are disconnected from each other. As comparison, Mem-W-56 and Mem-W-46 have macroporous structure with irregular big tear-like pores in the supporting layer and Mem-D has a dense structure with no observable pores. The quaternization temperature can also affect the membrane morphology. Mem-I-56 which underwent quaternization at 56°C has higher ion-exchange capacity (IEC) and smaller pores at top surface than Mem-I-46 which underwent quaternization at 46°C. Similarly, Mem-W-56 top surface has smaller pores than Mem-W-46.

The membranes are intended for DD application in this study, and hence some other related properties, including thermal and chemical stability, mechanical strength need to be explored and the results are discussed in the following sections.

3.2. Thermal stability

The TGA graphs, as shown in Fig. 3, are used to evaluate short-term thermal stability and provide information on the degradation patterns of the membranes. The membranes show similar mass loss trends, but the weight loss is different. In general, the whole degradation mode is divided into three stages. The initial stage before 100°C presenting a substantial decline is due to the evaporation of absorbed water. Mem-W-46 shows the most obvious weight loss in this stage due to its highest water uptake. Besides, Mem-D shows moderately lower weight loss in comparison with other membranes because of its non-porous structure and thus lower water content. Then, the second stage of weight loss, which can be attributed to the degradation of quaternary ammonium groups [31], appears in the range of 200°C–290°C with peak at ~230°C or ~260°C. Previous research reports that the commercial DF-120 membrane shows initial decomposition temperature of 202°C during this stage [27]. Hence, the thermal stability of the P84 co-polyimide membranes is similar to or higher than DF-120 membrane. When the temperature is close to 530°C, the third stage of rapid degradation of the polymer main chain occurs. As comparison, PPO-based membranes show degradation in this stage at the temperature of 380°C [44], which also confirms the higher thermal stability of the P84 co-polyimide membranes.

3.3. Chemical stability

Acid resistance plays an important role in the application of membranes in acidic solution. Accordingly, the weight changes of the P84 co-polyimide membranes are recorded

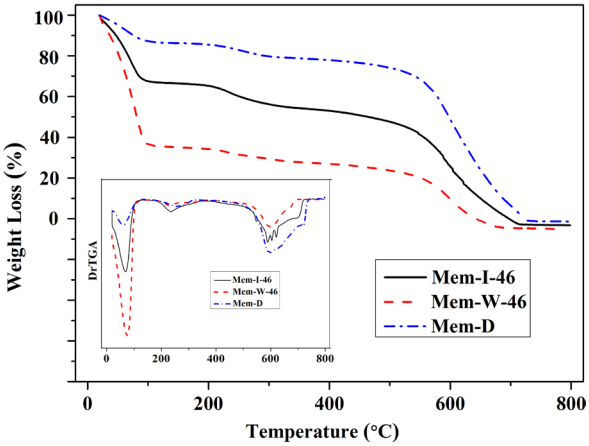

Fig. 3. Thermogravimetric analysis (TGA) thermograms and the first derivative of the TGA curve (DrTGA) of Mem-I-46, Mem-W-46 and Mem-D.

Table 2
Physicochemical properties of the P84 co-polyimide based membranes[a]

Membrane type	Thickness (mm)	Water uptake (%)	Area resistance (Ω cm²)	IEC (mmol/g)	PWP at 3 bar (×10⁻⁶ m³/(m² s))	Chemical stability[b] (%)
Mem-I-56	0.10	100	1.7	0.9	1.33	4.87
Mem-I-46	0.10	120	2.2	0.7	4.72	6.46
Mem-W-56	0.15	150	0.7	0.9	11.1	5.60
Mem-W-46	0.15	160	0.9	0.6	20	3.83
Mem-D	0.05	25	>80	0.3	–	5.07

[a]The data were cited from Zhang et al. [41] except the membrane thickness and chemical stability.
[b]The chemical stability was evaluated as the weight change (ΔW) after immersion in H_2SO_4 solution (1.0 mol/L) for 2 d at 25°C.

after immersion in H_2SO_4 solution (1.0 mol/L) for 2 d at 25°C, as shown in Table 2. The five membranes remain intact and flexible, and their weights show a slight increase, which is due to the swelling. The weight change of the membranes is similar, illustrating that the porous structure does not reduce the acid resistance.

3.4. Mechanical stability

The TS and elongation at break (E_b) values are shown in Fig. 4. TS values of porous membranes are in the range of 1.57–5.01 MPa, while E_b values are in the range of 3.11%–6.82%. The values are relatively low as compared with some reported values of dense membranes (7–16 MPa and 18%–123% [45]; 20–27 MPa and 4%–47% [46]), which should be mainly due to the porous structure. Mem-I-56 shows lower E_b value than Mem-I-46, and Mem-W-56 shows lower value than Mem-W-46. Mem-I-56 and Mem-W-56 are quaternized under higher temperature, and thus the grafted ethyl groups are enhanced [41]. Previous research has shown that the massive groups can make polymer chain segments stiffer and the relaxation of chain segments more difficult [47], and hence the membrane flexibility is decreased. Mem-D shows lower E_b value than most of the porous membranes, which is attributed to higher compactness and stiffness of the dense membrane [48].

3.5. Membrane cost estimation

In this experiment, the effective area of a single membrane was 20 cm^2, which was used as a base to estimate the membrane price. Considering the cost of P84 co-polyimide raw material ($176/kg) and reagent consumption but excluding electricity, waste disposal fee and labor cost, the rough cost for the final membrane was $0.383/20 cm^2 (IPA as the non-solvent) or $0.304/20 cm^2 (water as the non-solvent) if produced by the laboratory. It should be noted that the membrane cost of actual industrial production will be significantly reduced, for two reasons: (1) the price of raw material unit quality will decrease significantly; (2) the non-solvent bath (IPA or water) may be continuously utilized. However, additional costs will be added, including equipment investment, labor costs and disposal of waste liquids.

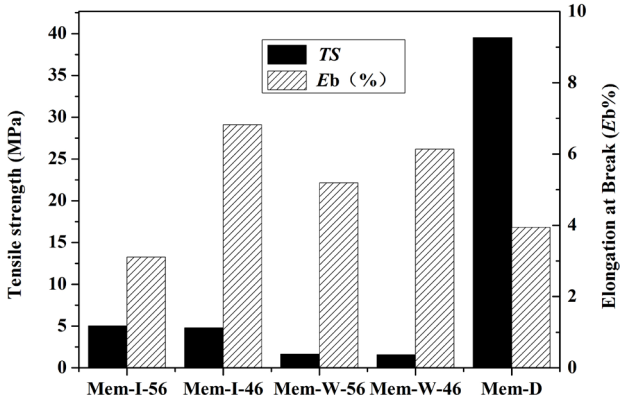

Fig. 4. Tensile strength (TS) and elongation at break (E_b) of the P84 co-polyimide based membranes.

3.6. Diffusion dialysis for $H_2SO_4/FeSO_4$ solution

3.6.1. Proton dialysis coefficient (U_H) with respect to the temperature

The DD performance is evaluated by U_H and separation factor (S). A simulated titanium white waste acid ($H_2SO_4/FeSO_4$) is used as the feed solution to evaluate the potential applications of porous P84 co-polyimide membranes in inorganic acids recovery. The DD is running at different temperatures (15°C–45°C) to optimize the operating conditions, as shown in Fig. 5. The U_H values increase significantly with the temperature. The increasing temperature accelerates the ions transport rate, and the diffusivity of ions is enhanced accordingly. As has been reported previously, in the case of strong acids, the ultimate hydrogen ion transmission rate is controlled by diffusion rate, rather than adsorption solubility [49]. Therefore, the U_H values increase at higher running temperature.

In addition, membrane swelling also governs the ion transportation [50]. The membrane swelling increases with the temperature, which promotes the ions migration inside the membrane, so the ions are more readily to pass through the membranes [46]. The U_H values for porous membranes are in the range of 0.00584–0.00781 m/h at 25°C, higher than that of S203 membrane (0.0018 m/h at 25°C) [23] and DF-120 membrane (0.00234 m/h at 25°C) [26]. The U_H values for porous membranes are 0.0036–0.0126 m/h for the temperature range of 15°C–45°C. Nevertheless, Mem-D gets the lowest U_H of 0.00001–0.00012 m/h and hence is not suitable for H_2SO_4 recovery. The dense structure and lower IEC value of Mem-D will incur a higher resistance for the passage of ions than that of porous structure. What's more, Fe^{2+} ion with larger size is more hindered and so the selectivity is very high (S = 28.3–419.9).

Among the different porous membranes, Mem-W-56 and Mem-W-46 show higher U_H values (0.00617–0.0126 m/h) than Mem-I-56 and Mem-I-46 (0.0036–0.0125 m/h), implying that the pore size is also a dominant factor influencing the DD performances. Unlike Mem-W-56 or Mem-W-46 with irregular big tear-like pores, Mem-I-56 and Mem-I-46 have sponge-like structure and the morphology is less loose. Therefore, the resistance of ions through the membranes increases, leading to lower U_H values.

Besides, Mem-W-46 shows higher U_H value than Mem-W-56 at 15°C, 25°C and 45°C, and Mem-I-46 shows U_H value higher than Mem-I-56. These changing trends can be ascribed to both membrane morphology and IEC values. On one hand, Mem-I-56 has smaller pores at top surface than Mem-I-46, and Mem-W-56 top surface also has smaller pores than Mem-W-46 [41], which will incur a higher resistance for the ions passage. On the other hand, the IECs of Mem-I-56 and Mem-W-56 are higher than that of Mem-I-46 and Mem-W-46. It seems that the membrane pore size is more critical for acid transport and hence the U_H values of Mem-I-46 and Mem-W-46 can be higher.

3.6.2. Separation factor (S) with respect to the temperature

The S values of Mem-W-56 and Mem-W-46 are basically below 5 within 15°C–45°C. The S values of Mem-I-56 and Mem-I-46, however, are much higher and are obviously

influenced by the temperature. The *S* values are largely related to the membrane pore morphology. As discussed earlier, Mem-I-56 and Mem-I-46 exhibit sponge-like structure, while Mem-W-56 and Mem-W-46 contain irregular big tear-like pores. The physical model put forward in previous research [44] can be utilized here to demonstrate how acid permeates through the sponge-like and tear-like structures. There exist a large number of tear-like macrochannels in Mem-W-56 and Mem-W-46, which lead to a sharp rise in free volume and accelerate the ion transport rate in the supporting layer. This is also why the increase in temperature has little effect on the separation factor of Mem-W-56 and Mem-W-46 (Fig. 5). In contrast, Mem-I-56 and Mem-I-46 are full of micronsized pores which are disconnected from each other and separated by ultrathin walls with positive charges. The membrane selectivity is significantly improved because the sequential pore walls are equivalent to a multi-layered barrier, and can hinder the transport of multivalent ions (Fe^{2+}) more effectively [51,52]. Accordingly, the *S* values of Mem-I-56 and Mem-I-46 are always higher than those of Mem-W-56 and Mem-W-46.

The *S* values of Mem-I-56 decrease all along from 22.2 to 6.2, indicating that Fe^{2+} migration is more obviously accelerated at higher temperature as compared with H^+. As comparison, the values of Mem-I-46 increase first and then decrease at 45°C. Similar trend has been observed in previous reports [46] and can be explained as follows: as the temperature increases from 15°C to 35°C, the increased membrane free volume accelerates H^+ migration while Fe^{2+} can still be effectively blocked, leading to the increase of *S* values. However, when temperature reaches 45°C, the membranes structure is further loosened and weakened [46], the hindrance of the membranes to H^+ or Fe^{2+} ions is reduced, leading to more Fe^{2+} ions diffusion and the decrease of *S* value. Mem-D, as comparison, has the lowest IEC value and dense structure, which cause large resistance to either H^+ or Fe^{2+} ions through the membrane. At higher temperatures, H^+ ions migration is accelerated while Fe^{2+} ions transport are still effectively suppressed, leading to gradual increase of the *S* value (Fig. 5).

In summary, although a higher permeability can be achieved for macroporous structure (Mem-W-56 and Mem-W-46), membrane selectivity will be reduced. Meanwhile, the sponge-like structure (Mem-I-56 and Mem-I-46) remains advantageous for improving ion selectivity, hence they are more desirable for practical usage. The acid transport mechanism can be specified to explain this phenomenon. Counter ions (HSO_4^- or SO_4^{2-}) are facilitated to transport through the membrane by the presence of anion exchange groups ($-N^+(CH_2CH_3)_3$). For the preservation of electrical neutrality, cations (H^+ or Fe^{2+}) should transport to the diffusate side. The H^+ ions have higher competition in diffusion through the sponge-like micropores than Fe^{2+} ions because of their smaller size, lower valence state and higher mobility. Hence, they can preferentially be transported through Mem-I-56 and Mem-I-46 [44].

3.7. Water osmosis

Water osmosis is a natural phenomenon that water molecules move from a low concentration solution into a high concentration solution through a semipermeable membrane [53]. In this study, the diffusate compartment is filled with water and the dialysate compartment contains 0.9 mol/L H_2SO_4/0.3 mol/L $FeSO_4$ at the beginning of DD running. Hence, osmotic pressure is present to cause water osmosis. Previous study [40] about DD of HCl/glyphosate liquor has shown that water permeation is mainly caused by the different concentration of organic component across the membrane, rather than HCl. Similarly, we can also assume that the water osmosis in this work is mainly due to the presence of high concentration metal salts in the dialysate compartment, which can be further confirmed in subsequent section 3.8. Besides, the membranes contain hydrophilic quaternary ammonium groups and have porous structure, which may also accelerate the water permeation.

The water osmosis volume (V_{H_2O}) with respect to temperature is illustrated in Fig. 6. Mem-D has the lowest IEC value and dense structure and thus is more difficult to penetrate ions than the porous membranes. Hence, the water osmosis is difficult to occur, and V_{H_2O} is lower than 3 mL. The V_{H_2O} of Mem-I-56 and Mem-I-46 is generally similar and increases rapidly with the temperature. This may be related to the membrane structure: Mem-I-56 has a higher IEC while Mem-I-46 contains larger pore size at the top surface, both of which are advantageous for water permeability. Hence, the water

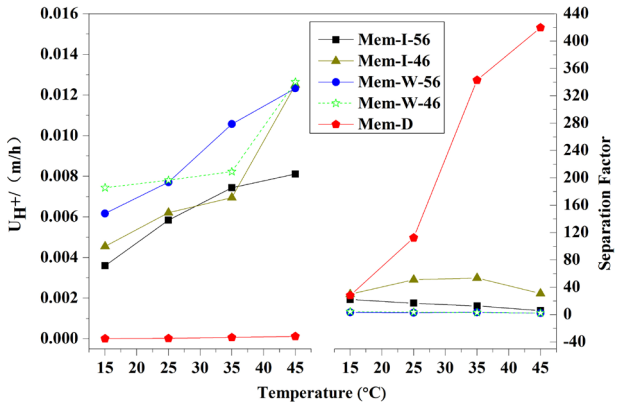

Fig. 5. Acid dialysis coefficients (U_H) and separation factor (*S*) at different temperatures for H_2SO_4/$FeSO_4$ mixture.

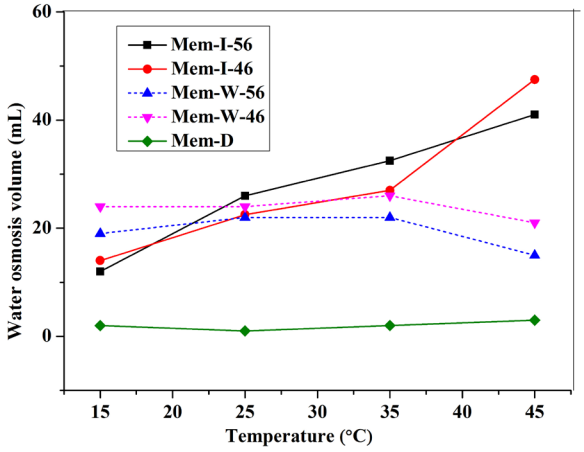

Fig. 6. Water osmosis volume (V_{H_2O}) during DD of H_2SO_4/$FeSO_4$ mixture with respect to the temperature.

permeability is similar. Meanwhile, the hydrophilic polymer chains can be swelled in water and their structure is loosened and water adsorption is facilitated at higher temperature [46]. Therefore, more water molecules are penetrated due to the enhancement of ions penetration.

However, Mem-W-56 and Mem-W-46 with tear-like pores have different change of water osmosis. The V_{H_2O} values are less affected by temperature and even decrease at 45°C. This can be attributed to the fact that Fe^{2+} ions migration is highly accelerated and the concentration difference of Fe^{2+} ions across the membranes is significantly reduced at higher temperature, causing the osmotic pressure to weaken. For example, at the end of experiment at 45°C, the concentration difference across Mem-W-56 is as follows: the dialysate compartment contains 0.169 mol/L Fe^{2+}, while the diffusate compartment contains 0.141 mol/L Fe^{2+} at the end of DD running. Obviously, the concentration difference of Fe^{2+} ions between the two compartments is decreased significantly, leading to significantly decreased V_{H_2O} value at high temperature.

3.8. DD performance for pure acetic acid

HAc is a type of weak acid and thus is difficult to transport through the membranes. Besides, HAc is corrosive and hence the DD process of HAc is still rare in practical application. Nevertheless, the P84 co-polyimide membranes showed good resistance for DD process of HAc and remained intact and flexible after running 4 d, each day running continuously for 5 h. Here porous membrane Mem-I-46, due to its high permeability and high selectivity, is attempted to transport pure HAc solution (0.9 mol/L). The dialysis coefficient of HAc (U_{HAc}) increases from 0.00239 to 0.0133 m/h as the temperature increases from 15°C to 45°C, as shown in Fig. 7. The higher temperature accelerates the Ac^- ion passage through the porous membrane, and so more H^+ ion needs to be transported to the dialysate side to preserve the electrical neutrality. Meanwhile, the V_{H_2O} is only ~3 mL, which is much lower than those of previous H_2SO_4/$FeSO_4$ mixture, and is not obviously affected by temperature. This confirms our previous assumption that the water permeation should be mainly associated with the concentration difference of metal salts rather than acids.

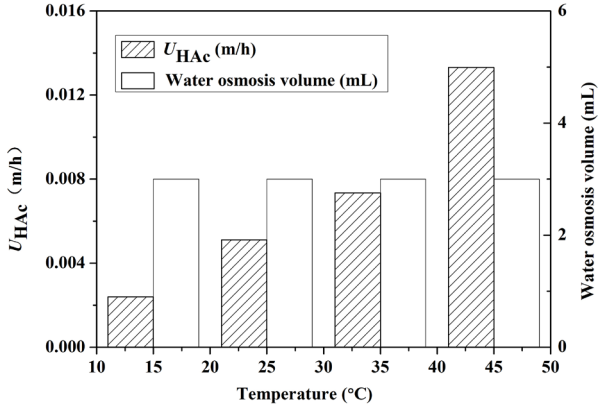

Fig. 7. DD performance of Mem-I-46 for pure HAc solution, including the dialysis coefficient of HAc (U_{HAc}) and water osmosis volume (V_{H_2O}).

In addition, Mem-I-46 maintains excellent flexibility at the end of the experiment, indicating its higher stability than the commercial membrane DF-120 which can be partly dissolved in HAc solution [27]. The U_{HAc} is 0.00511 m/h at 25°C, similar to the values (0.0034–0.0091 m/h) of the previously reported polyvinyl alcohol (PVA)/SiO_2 hybrid AEMs [25]. Nevertheless, the hybrid AEM has PVA as the membrane matrix, which is prone to high swelling and thus not suitable to be used at elevated temperatures. Hence, the U_{HAc} of Mem-I-46 is acceptable considering the usage of P84 matrix of much more hydrophobic nature.

4. Conclusions

P84 co-polyimide porous AEMs are prepared by phase inversion using IPA or water as the non-solvent, followed by amination and quaternization. The membranes prepared from IPA show a sponge-like structure while the membranes prepared from water contain irregular big tear-like pores. The membranes are stable in H_2SO_4 solution, and have short-term thermal stability higher than 200°C.

Porous membranes are then used in DD to separate a mixture of H_2SO_4 and $FeSO_4$ solution. The acid dialysis coefficients (U_H) increase with the temperature. Membranes with tear-like porous structures show higher U_H than the membranes with sponge-like porous structures. However, sponge-like structure membranes show higher separation factors (S) because of its multi-layered barricade to distinguish protons from multivalent ions. The dense membrane gets the lowest U_H of 0.00001–0.00012 m/h and hence is not suitable for H_2SO_4 recovery. The Mem-I-46 shows excellent U_H (0.0069 m/h) and maximum S (53.8) for H_2SO_4 at 35°C and exhibits U_{HAc} in the range of 0.00239–0.0133 m/h for pure HAc solution. Meanwhile, the water osmosis phenomenon is obvious during DD of H_2SO_4/$FeSO_4$ solution and increases with the temperature because of the osmosis pressure induced by the concentration difference of Fe^{2+} ions across the membrane. The water osmosis for pure HAc is much less and remains nearly unchanged (~3 mL) with temperature. On the whole, the porous structure can reduce the transport resistance through the membrane and are favorable for the recovery of acids.

Acknowledgment

This project was supported by the National Science Foundation of China (Nos. 21476056, 21606063 and 21376204).

References

[1] J. Jeong, M.S. Kim, B.S. Kim, S.K. Kim, W.B. Kim, J.C. Lee, Recovery of H_2SO_4 from waste acid solution by a diffusion dialysis method, J. Hazard. Mater., 124 (2005) 230–235.
[2] A. Agrawal, K.K. Sahu, An overview of the recovery of acid from spent acidic solutions from steel and electroplating industries, J. Hazard. Mater., 171 (2009) 61–75.
[3] P. Rudnicki, Z. Hubicki, D. Kołodyńska, Evaluation of heavy metal ions removal from acidic waste water streams, Chem. Eng. J., 252 (2014) 362–373.
[4] X. Feng, L.Y. Jiang, Y. Song, Titanium white sulfuric acid concentration by direct contact membrane distillation, Chem. Eng. J., 285 (2016) 101–111.

[5] C.X. Tian, Effects of hydrolysis parameters on TiO_2 white pigment from low concentration industrial $TiOSO_4$ solution via sulfate process, Adv. Mater. Res., 602–604 (2013) 1243–1249.
[6] C.X. Tian, S.H. Huang, Y. Yang, Anatase TiO_2 white pigment production from unenriched industrial titanyl sulfate solution via short sulfate process, Dyes Pigm., 96 (2013) 609–613.
[7] A. Salvador, M.C. Pascual-Martí, J.R. Adell, A. Requeni, J.G. March, Analytical methodologies for atomic spectrometric determination of metallic oxides in UV sunscreen creams, J. Pharm. Biomed. Anal., 22 (2000) 301–306.
[8] C.Y. Su, H.Z. Tang, K. Chu, C.K. Lin, Cosmetic properties of TiO_2/mica-BN composite powder prepared by spray drying, Ceram. Int., 40 (2014) 6903–6911.
[9] P.S. Croce, A. Mousavi, A sustainable sulfate process to produce TiO_2 pigments, Environ. Chem. Lett., 11 (2013) 325–328.
[10] Q.F. Wei, X.L. Ren, J.J. Guo, Y.X. Chen, Recovery and separation of sulfuric acid and iron from dilute acidic sulfate effluent and waste sulfuric acid by solvent extraction and stripping, J. Hazard. Mater., 304 (2016) 1–9.
[11] C.H. Huang, T.W. Xu, Y.P. Zhang, Y.H. Xue, G.W. Chen, Application of electrodialysis to the production of organic acids: state-of-the-art and recent developments, J. Membr. Sci., 288 (2007) 1–12.
[12] H. Takahashi, K. Ohba, K.I. Kikuchi, Sorption of monocarboxylic acids by an anion-exchange membrane, Biochem. Eng. J., 16 (2003) 311–315.
[13] M. Bailly, Production of organic acids by bipolar electrodialysis: realizations and perspectives, Desalination, 144 (2002) 157–162.
[14] M. Bailly, H.R.D. Balmann, P. Aimar, F. Lutin, M. Cheryan, Production processes of fermented organic acids targeted around membrane operations: design of the concentration step by conventional electrodialysis, J. Membr. Sci., 191 (2001) 129–142.
[15] M. Tomaszewska, M. Gryta, A.W. Morawski, Recovery of hydrochloric acid from metal pickling solutions by membrane distillation, Sep. Purif. Technol., 22–23 (2001) 591–600.
[16] S.C. Wu, Z.M. Cheng, S.D. Wang, X.L. Shan, Recovery of terephthalic acid from alkali reduction wastewater by cooling crystallization, Chem. Eng. Technol., 34 (2011) 1614–1618.
[17] V. Nenov, N. Dimitrova, I. Dobrevsky, Recovery of sulphuric acid from waste aqueous solutions containing arsenic by ion exchange, Hydrometallurgy, 44 (1997) 43–52.
[18] C.H. Shin, J.Y. Kim, J.Y. Kim, H.S. Kim, H.S. Lee, D. Mohapatra, J.W. Ahn, J.G. Ahn, W. Bae, A solvent extraction approach to recover acetic acid from mixed waste acids produced during semiconductor wafer process, J. Hazard. Mater., 162 (2009) 1278–1284.
[19] L. Cifuentes, I. García, P. Arriagada, J.M. Casas, The use of electrodialysis for metal separation and water recovery from $CuSO_4$-H_2SO_4-Fe solutions, Sep. Purif. Technol., 68 (2009) 105–108.
[20] J. Xu, S.G. Lu, D. Fu, Recovery of hydrochloric acid from the waste acid solution by diffusion dialysis, J. Hazard. Mater., 165 (2009) 832–837.
[21] X. Zhang, X.L. Wang, C.R. Li, H.Y. Feng, Y.M. Wang, J.Y. Luo, T.W. Xu, A quantification of diffusion dialysis process: single electrolyte system (sodium chloride solution), Sep. Purif. Technol., 105 (2013) 48–54.
[22] J.Y. Luo, C.M. Wu, T.W. Xu, Y.H. Wu, Diffusion dialysis-concept, principle and applications, J. Membr. Sci., 366 (2011) 1–16.
[23] T.W. Xu, W.H. Yang, Sulfuric acid recovery from titanium white (pigment) waste liquor using diffusion dialysis with a new series of anion exchange membranes — static runs, J. Membr. Sci., 183 (2001) 193–200.
[24] Z. Palatý, H. Bendová, Separation of HCl+$FeCl_2$ mixture by anion-exchange membrane, Sep. Purif. Technol., 66 (2009) 45–50.
[25] C.M. Wu, Y.H. Wu, J.Y. Luo, T.W. Xu, Y.X. Fu, Anion exchange hybrid membranes from PVA and multi-alkoxy silicon copolymer tailored for diffusion dialysis process, J. Membr. Sci., 356 (2010) 96–104.
[26] J.J. Tang, K.G. Zhou, Q.X. Zhang, Sulfuric acid recovery from rare earth sulphate solutions by diffusion dialysis, Trans. Nonferrous. Met. Soc. China, 16 (2006) 951–955.
[27] Y.H. Wu, J.Y. Luo, L.L. Yao, C.M. Wu, F.L. Mao, T.W. Xu, PVA/SiO_2 anion exchange hybrid membranes from multisilicon copolymers with two types of molecular weights, J. Membr. Sci., 399–400 (2012) 16–27.
[28] F.J. Sun, C.M. Wu, Y.H. Wu, T.W. Xu, Porous BPPO-based membranes modified by multisilicon copolymer for application in diffusion dialysis, J. Membr. Sci., 450 (2014) 103–110.
[29] X.C. Lin, E. Shamsaei, B. Kong, J.Z. Liu, Y.X. Hu, T.W. Xu, H.T. Wang, Porous diffusion dialysis membranes for rapid acid recovery, J. Membr. Sci., 502 (2016) 76–83.
[30] X.C. Lin, S. Kim, D.M. Zhu, E. Shamsaei, T.W. Xu, X.Y. Fang, H.T. Wang, Preparation of porous diffusion dialysis membranes by functionalization of polysulfone for acid recovery, J. Membr. Sci., 524 (2017) 557–564.
[31] X.C. Lin, E. Shamsaei, B. Kong, J.Z. Liu, T.W. Xu, H.T. Wang, Fabrication of asymmetrical diffusion dialysis membranes for rapid acid recovery with high purity, J. Mater. Chem. A, 4 (2016) 8478–8478.
[32] S. Kim, K.S. Jang, H.D. Choi, S.H. Choi, S.J. Kwon, I.D. Kim, J.A. Lim, J.M. Hong, Porous polyimide membranes prepared by wet phase inversion for use in low dielectric applications, Int. J. Mol. Sci., 14 (2013) 8698.
[33] K. Vanherck, G. Koeckelberghs, I.F.J. Vankelecom, Crosslinking polyimides for membrane applications: a review, Prog. Polym. Sci., 38 (2013) 874–896.
[34] P.S. Tin, T.S. Chung, Y. Liu, R. Wang, S.L. Liu, K.P. Pramoda, Effects of cross-linking modification on gas separation performance of Matrimid membranes, J. Membr. Sci., 225 (2003) 77–90.
[35] W.Y. Xu, D.R. Paul, W.J. Koros, Carboxylic acid containing polyimides for pervaporation separations of toluene/iso-octane mixtures, J. Membr. Sci., 219 (2003) 89–102.
[36] N.L. Le, Y. Wang, T.S. Chung, Synthesis, cross-linking modifications of 6FDA-NDA/DABA polyimide membranes for ethanol dehydration via pervaporation, J. Membr. Sci., 415–416 (2012) 109–121.
[37] I.C. Kim, J.H. Kim, K.H. Lee, T.M. Tak, Phospholipids separation (degumming) from crude vegetable oil by polyimide ultrafiltration membrane, J. Membr. Sci., 205 (2002) 113–123.
[38] C.Y. Ba, J. Langer, J. Economy, Chemical modification of P84 copolyimide membranes by polyethylenimine for nanofiltration, J. Membr. Sci., 327 (2009) 49–58.
[39] J.H. Cheng, Y.C. Xiao, C.M. Wu, T.S. Chung, Chemical modification of P84 polyimide as anion-exchange membranes in a free-flow isoelectric focusing system for protein separation, Chem. Eng. J., 160 (2010) 340–350.
[40] Y.H. Wu, P.F. Wang, G.C. Zhang, C.M. Wu, Water osmosis in separating acidic HCl/glyphosate liquor by continuous diffusion dialysis, Sep. Purif. Technol., 179 (2017) 86–93.
[41] C.Y. Zhang, S. Xue, G.S. Wang, C.M. Wu, Y.H. Wu, Production of lactobionic acid by BMED process using porous P84 co-polyimide anion exchange membranes, Sep. Purif. Technol., 173 (2016) 174–182.
[42] W. Li, Y.M. Zhang, J. Huang, X.B. Zhu, Y. Wang, Separation and recovery of sulfuric acid from acidic vanadium leaching solution by diffusion dialysis, Sep. Purif. Technol., 96 (2012) 44–49.
[43] M.I. Khan, A.N. Mondal, C.L. Cheng, J.F. Pan, K. Emmanuel, L. Wu, T.W. Xu, Porous BPPO-based membranes modified by aromatic amine for acid recovery, Sep. Purif. Technol., 157 (2016) 27–34.
[44] L. Ge, A.N. Mondal, X.H. Liu, B. Wu, D.B. Yu, Q.H. Li, J.B. Miao, Q.Q. Ge, T.W. Xu, Advanced charged porous membranes with ultrahigh selectivity and permeability for acid recovery, J. Membr. Sci., 536 (2017) 1
[45] D.S. Kim, H.B. Park, Y.M. Lee, Y.H. Park, J.W. Rhim, Preparation and characterization of PVDF/silica hybrid membranes containing sulfonic acid groups, J. Appl. Polym. Sci., 93 (2004) 209–218.

[46] J.Y. Luo, C.M. Wu, Y.H. Wu, T.W. Xu, Diffusion dialysis of hydrochloride acid at different temperatures using PPO–SiO_2 hybrid anion exchange membranes, J. Membr. Sci., 347 (2010) 240–249.
[47] A.N. Mondal, C.L. Zheng, C.L. Cheng, M.M. Hossain, M.I. Khan, Z.L. Yao, L. Wu, T.W. Xu, Effect of novel polysiloxane functionalized poly(AMPS-co-CEA) membranes for base recovery from alkaline waste solutions via diffusion dialysis, RSC Adv., 5 (2015) 95256–95267.
[48] M. Irfan, N.U. Afsar, E. Bakangura, A.N. Mondal, M.I. Khan, K. Emmanuel, Z.J. Yang, L. Wu, T.W. Xu, Development of novel PVA-QUDAP based anion exchange membranes for diffusion dialysis and theoretical analysis therein, Sep. Purif. Technol., 178 (2017) 269–278.
[49] A. Narębska, M. Staniszewski, Separation of fermentation products by membrane techniques. I. Separation of lactic acid/lactates by diffusion dialysis, Sep. Sci. Technol., 32 (1997) 1669–1682.
[50] Y.B. He, J.F. Pan, L. Wu, L. Ge, T.W. Xu, Facile preparation of 1,8-diazabicyclo[5.4.0] undec-7-ene based high performance anion exchange membranes for diffusion dialysis applications, J. Membr. Sci., 491 (2015) 45–52.
[51] Y.Y. Zhao, M.R. Li, Z.Z. Yuan, X.F. Li, H.M. Zhang, I.F.J. Vankelecom, Advanced charged sponge-like membrane with ultrahigh stability and selectivity for vanadium flow batteries, Adv. Funct. Mater., 26 (2016) 210–218.
[52] H.Z. Zhang, H.M. Zhang, F.X. Zhang, X.F. Li, Y. Li, I. Vankelecom, Advanced charged membranes with highly symmetric spongy structures for vanadium flow battery application, Energy Environ. Sci., 6 (2013) 776–781.
[53] L.R. Valladares, Z. Li, S. Sarp, S.S. Bucs, G. Amy, J.S. Vrouwenvelder, Forward osmosis niches in seawater desalination and wastewater reuse, Water Res., 66 (2014) 122–139.